PERGAMON

Radiation Measurements 33 (2001) 229–234

Radiation Measurements

www.elsevier.com/locate/radmeas

Predictions of secondary neutrons and their importance to radiation effects inside the international space station

T.W. Armstrong *, B.L. Colborn

Science Applications International Corporation (SAIC), 1706 Prospect Road, Prospect TN 38477, USA

Received 1 November 1999; accepted 18 January 2000

1. Introduction

As part of a study funded by NASA MSFC to assess the contribution of secondary particles in producing radiation damage to optoelectronics devices located on the International Space Station (ISS), Monte Carlo calculations have been made to predict secondary spectra vs. shielding inside ISS modules and in electronics boxes attached on the truss (Armstrong and Colborn, 1998). The calculations take into account secondary neutron, proton, and charged pion production from the ambient galactic cosmic-ray (GCR) proton, trapped proton, and neutron albedo environments. Comparisons of the predicted neutron spectra with measurements made on the Mir space station and other spacecraft have also been made (Armstrong and Colborn, 1998).

In this paper, some initial results from folding the predicted neutron spectrum inside ISS modules from Armstrong and Colborn (1998) with several types of radiation effects response functions related to electronics damage and astronaut-dose are given. These results provide an estimate of the practical importance of neutrons compared to protons in assessing radiation effects for the ISS. Also, the important neutron energy ranges for producing these effects have been estimated, which provides guidance for onboard neutron measurement requirements.

2. Methods

The ISS secondary neutron calculations (Armstrong and Colborn, 1998) were made using the SAIC version of the HETC high-energy Monte Carlo radiation transport code, which determines secondary particle production from spallation collisions by using a two-step intranuclear-cascade-evaporation nuclear model. Low-energy ($\leqslant 20$ MeV) neutrons are transported using the MORSE Monte Carlo code, which employs cross sections from the ENDF data base to transport neutrons down to thermal energies.

A simplified shielding model was used for the radiation transport calculations: ISS modules were modeled as a long (100 m), hollow cylinder (outer radius of 280 cm, internal void radius of 100 cm, with the radial areal density of 20.7 g/cm^2 comprised of reduced-density aluminum). This simple model is derived from a detailed 3-D mass model of the ISS which has been developed for ionizing radiation analyses (Colborn et al., 1995). Additional details and assumptions for the calculational procedure are given in Armstrong and Colborn (1998).

3. Results

3.1. Induced neutron spectra inside ISS modules

Fig. 1 shows the calculated orbit-average differential neutron, proton, and charged pion spectra inside ISS modules due to the ambient GCR proton, trapped proton, and Earth neutron albedo environments. Fig. 2 shows integral particle spectra corresponding to the differential spectra in Fig. 1. The baseline parameters used for determining radiation exposure were 500 km altitude, 51.6° inclination, and solar maximum conditions, which are the parameters specified by NASA in determining the ionizing radiation environment definition for radiation design purposes (Johnson Space Flight Center, 1994). Approximate scaling factors for estimating neutron spectra for other altitudes and solar minimum conditions are discussed in Armstrong and Colborn (1998).

* Corresponding author.

PII: S1350-4487(00)00152-9

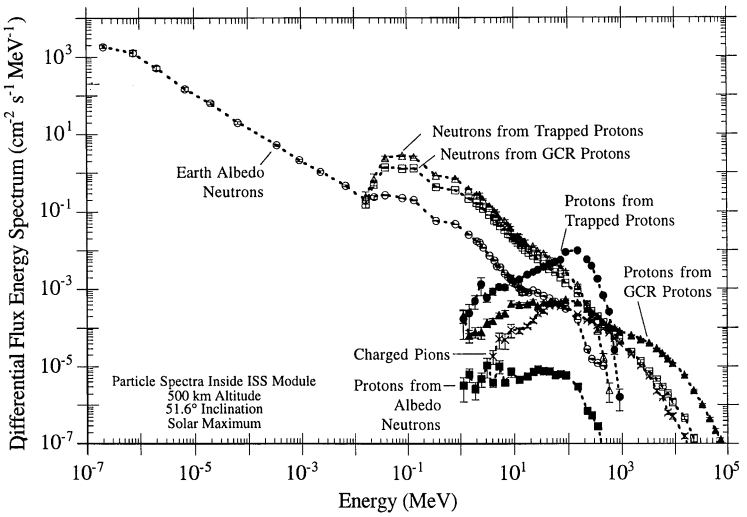

Fig. 1. Predicted differential particle spectra inside ISS modules.

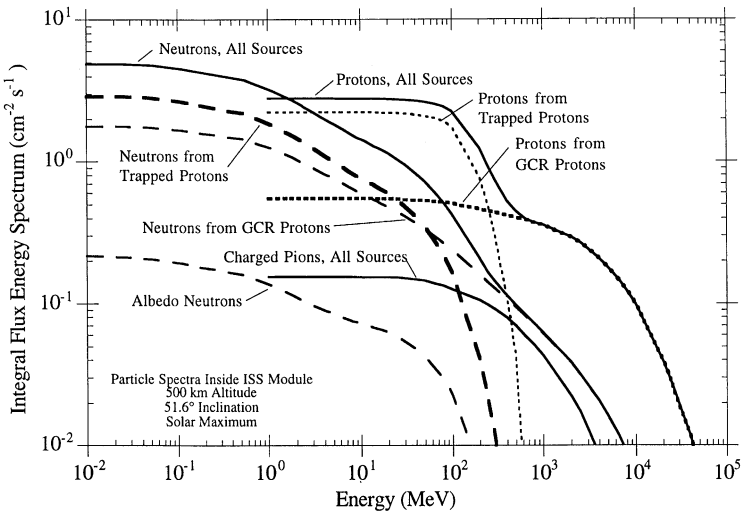

Fig. 2. Predicted integral particle spectra inside ISS modules.

The results of Fig. 1 show that below ≈ 10 keV the neutron spectrum is dominated by albedo neutrons; in the energy range from 10 keV to 100 MeV, secondary neutrons from trapped protons and GCR protons contributed about equally; and GCR-induced neutrons dominate above 100 MeV. (While the trapped proton vs. GCR proton contribution to the induced neutron flux is approximately the same here, the relative contribution depends on numerous factors — such as altitude, inclination, and shielding — so the near-equality of the two contributions obtained here does not necessarily hold for other orbits.)

Fig. 1 indicates that there is a local minimum in the total neutron spectrum (sum of albedo, trapped, and GCR components) at ≈ 10 keV and a local maximum at ≈ 100 keV. The energy and existence of this local minimum in the neutron spectrum is expected to be sensitive to material composition in the vicinity of the spatial point of interest. In the present calculations, only aluminum was used as the shielding material; for locations containing substantial amounts of lower atomic weight (particularly hydrogenous) materials with more efficient neutron moderation properties, this local minimum may shift to lower energies or disappear.

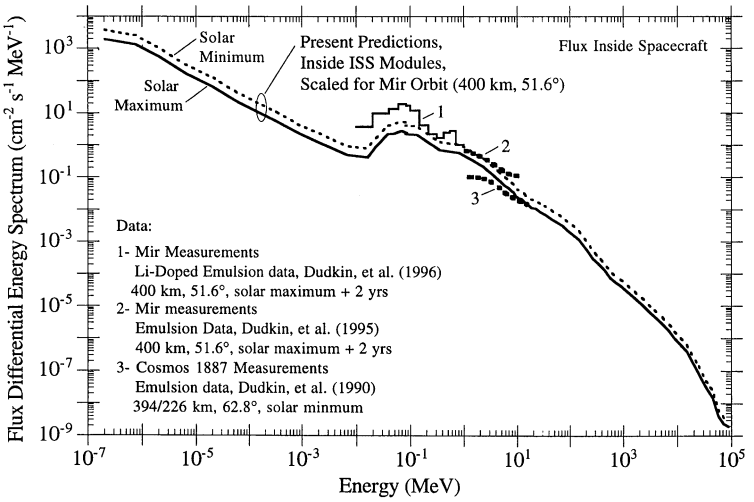

Fig. 3. Comparison of ISS predicted neutron spectra with measurements inside the Mir space station (Dudkin et al., 1996) and Cosmos 1887 spacecraft (Dudkin et al., 1990).

3.2. Comparison of predicted neutron spectra with flight data

The predicted ISS neutron spectra have been compared with several sets of neutron data from Mir, the Salyut 7 - Cosmos 1686 orbital station, and Cosmos satellite measurements (Armstrong and Colborn, 1998). Fig. 3 shows predicted neutron spectra compared to emulsion measurements made on Mir (Dudkin et al., 1996) and Cosmos 1887 (Dudkin et al., 1990). In the energy range from $\approx$200 keV to 15 MeV, agreement with the Mir data is quite good, better than a factor of two. For the lower energy measurement range of 10–200 keV, the measured flux is considerably higher than predicted, by a factor of about three near 100 keV. Both measurements and predictions exhibit a local maximum in the spectrum at about 100 keV. Additional comparisons with flight data, as well as additional results from the ISS neutron calculations, are given in Armstrong and Colborn (1998).

It is important to note that shielding distributions for the flight neutron measurements are not available; thus, differences between the ISS shielding used in the calculations and the shielding for the measurement locations are expected to account for some of the differences in Fig. 3 between predicted and measured neutron spectra.

3.3. Neutron contribution to radiation effects

The neutron and proton spectra in Fig. 1 have been integrated over several different radiation effects response functions related to electronics damage and astronaut dose to obtain the contribution of neutrons vs. protons in producing such effects. The results are shown in Table 1 in terms of the neutron contribution to the total (neutron plus proton) induced effect. For the electronics total dose and displacement damage estimates, response functions from Griffin et al. (1991), Dale et al. (1994, preprint) and Burke et al. (1988) were used. As a rough estimate of the neutron contribution to single-event effects (SEE) produced in microelectronics, neutron and proton nonelastic interaction cross sections for silicon (National Nuclear Data Center; Tripathi et al., 1996) were used, which is expected to be a reasonable approximation for devices having low thresholds for upset. For estimating the neutron contribution to the absorbed dose and dose-equivalent in tissue, response functions from ICRP-51 (ICRP Publication 51, 1987) based on neutrons and protons incident normally on a 30-cm slab of tissue were used.

Table 1 indicates that, as expected, for dose effects where the energy deposition is dominated by ionization, neutrons make only a small ($\leqslant$ 10%) contribution. However, for the other effects, which depend on nuclear interactions and their products, the neutron contribution is significant and comparable to the proton contribution in most cases. Table 1 also shows that for this particular orbit and shielding configuration, and for the radiation effects considered, neutrons from GCR protons and trapped protons contribute about equally. Albedo neutrons are not important for the effects considered, although for some situations, such as backgrounds to radiation-sensitive instrumentation and sensors, the inelastic and capture gamma rays produced by albedo neutrons may be important (e.g., Armstrong et al., 1998).

The neutron contribution to radiation effects obtained here for SEE and dose-equivalent should be regarded as scoping estimates because only approximate response functions have been used for these initial estimates. Improved estimates based on measured neutron and proton cross sections for particular types of single-event mechanisms and a variety

Table 1
Contribution of neutrons to radiation effects inside ISS modules (500 km altitude, 51.6° inclination orbit at solar maximum)

	Neutrons from GCR protons (%)	Neutrons from trapped protons (%)	Neutrons from earth albedo (%)	Neutrons from all sources (%)
Electronics effects				
Dose in Si	0.60	0.51	0.04	1.1
Displacement damage in Si	24	35	2	62
Displacement damage in GaAs	18	23	2	43
Single-event effects[a]	25	34	2	62
Effects in tissue[b,c]				
Absorbed dose, at max depth	2	2	0.1	4
Absorbed dose, at 10 mm depth	4	5	0.4	10
Dose equivalent, at max depth	9	11	1	21
Dose equivalent, at 10 mm depth	21	26	2	49

[a]Based on nonelastic nuclear cross sections for silicon.
[b]For normal incidence on 30 cm tissue slab.
[c]Using ICRP 51 flux-to-dose factors with pre-1985 neutron QF × 2.

of different device sensitivities are needed to definitively characterize the neutron contribution to SEE. Also, more recent and extensive sets of flux-to-dose factors are available for estimating the neutron contribution to biological effects in terms of dose-equivalent compared to the factors used here.

3.4. Important secondary neutron energies

To obtain a measure of the important neutron energies in producing a particular radiation effect ($\mathscr{E}$), the effect calculation is written as

$$\mathscr{E} = \int \phi(E)R(E)\,\mathrm{d}E = \int I(E)\,\mathrm{d}(\ln E),$$

where $\phi(E)$ is the neutron differential flux spectrum, $R(E)$ is the response function for the effect, and $I(E) \equiv \phi(E)R(E)$. In discrete form

$$\mathscr{E} = \sum_i I_i \ln\left(\frac{E_{i+1}}{E_i}\right) = c\sum_i I_i$$

for a constant $\ln E$ grid.

Fig. 4 shows plots of I_i, normalized to unity at maximum value, vs. logarithm of neutron energy for several radiation effects. Fig. 4 shows that neutron-induced displacement damage and SEE in silicon are produced mainly by neutrons in the 1–10 MeV energy range, whereas for displacement damage in gallium arsenide neutrons < 1 and > 10 MeV also make significant contributions. For tissue dose-equivalent, neutrons from ≈ 100 keV up to ≈ 1 GeV are important. The neutron contribution within broad energy ranges is shown in Table 2.

4. Conclusions

The secondary-neutron spectrum inside ISS modules has been predicted over the energy range from 10^{-7} to 10^{5} MeV using Monte Carlo radiation transport methods that take into account the details of secondary particle production and transport. These results for the internal radiation environment induced by the GCR proton, trapped proton, and albedo neutron external environment allow estimates of the neutron contribution to radiation effects, and the important neutron energies for such effects, to be estimated for the ISS.

The predicted neutron spectrum for the ISS is in reasonable agreement with Mir measurements and several other sets of flight data that have been compared with Armstrong and Colborn (1998). While these comparisons give agreement between predictions and measurements within about a factor of ±2, this should not be interpreted as the accuracy obtainable for the Monte Carlo methods used because the shielding distributions for the measurements are generally not known and, therefore, cannot be properly accounted for in the calculations; also, large uncertainties are usually associated with currently available neutron flight data. Thus, prediction accuracies better than a factor of two are expected when the measurement conditions are well known and simulated in detail. Additional flight data using neutron dosimeters with well-established responses over a wide energy range, and with well-defined shielding distributions for measurement locations, are needed to realize definitive quantitative assessments of predictive models and methods for secondary-neutron spectra in spacecraft.

The estimates here on the importance of secondary neutrons to several types of radiation effects indicate that for effects dominated by nuclear interactions (e.g., displacement damage and single-event effects in microelectronics, biological dose-equivalent) the secondary neutrons contribute

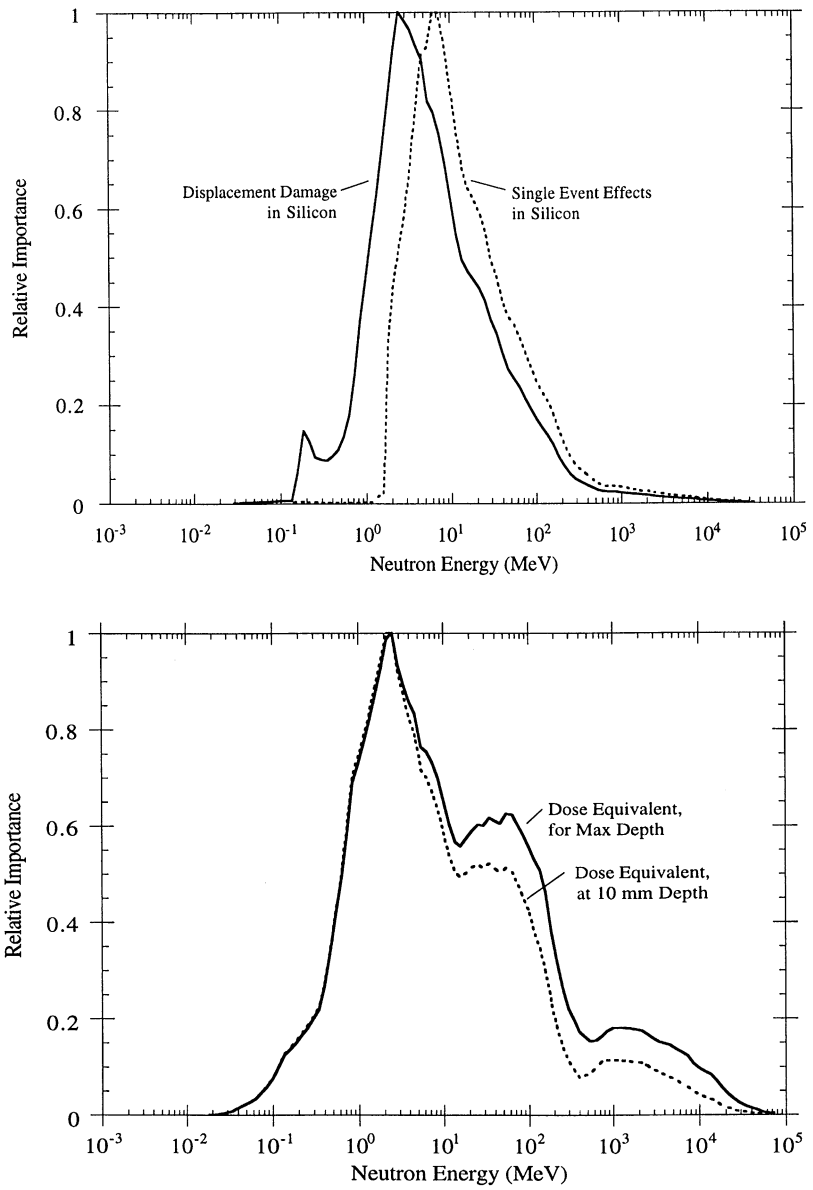

Fig. 4. Importance of neutron energy in producing radiation effects in silicon (top graph) and dose equivalent in tissue (bottom graph).

Table 2
Contribution of neutrons by energy range to radiation effects

Neutron energy range (MeV)	Electronics effects			Effects in tissue	
	Displacement damage in Si (%)	Displacement damage in GaAs (%)	Single-event effects (%)	Dose equivalent max depth (%)	Dose equivalent 10 mm depth (%)
< 0.1	0	1	0	1	1
0.1–1	9	14	0	13	15
1–10	58	33	46	38	43
10–100	27	31	42	27	26
> 100	6	22	11	22	15

about 40–60% of the total (neutron plus proton) induced effects. While this is higher than the contribution generally attributed previously to neutrons based on flight measurements, the larger contribution obtained here does not seem unreasonable in view of the large mass presented by the ISS for secondary neutron generation.

The important neutron energy ranges for several types of radiation effects have been estimated, which provides guidance on the energy range capabilities needed for onboard neutron monitors. For the low-energy limit, measurements down to ≈ 100 keV are generally needed. For the high end, measurements up to at least 100 MeV are needed, and for some effects the neutron contribution > 100 MeV is appreciable (see Table 2).

Acknowledgements

This work was performed under contract NAS8-98202 from the NASA Marshall Space Flight Center, J.W. Watts, Jr. contract technical representative.

References

Armstrong, T.W., Colborn, B.L., 1998. Predictions of secondary neutron and proton fluxes induced in the International Space Station by the space radiation environment. Science Applications International Corporation Report No. 98042R (NASA/MSFC Contractor Report), August 1998.

Armstrong, T.W., Colborn, B.L., Dietz, K.L., Ramsey, B.D., 1998. Neutron induced background in the MIXE X-ray detector at balloon altitudes. 1997 Conference on the High Energy Radiation Background in Space, ISBN 0-7803-4335-2.

Burke, E.A. et al., 1988. Energy dependence of proton-induced displacement damage in GaAs. IEEE Trans. Nucl. Sci. 34, 1220.

Colborn, B.L., Ringler, S.J., Armstrong, T.W., 1995. CADrays 3-D mass model of International Space Station alpha: interim version through flight assembly stage 19A. Science Applications International Corp. Report SAIC-TN-9528 (NASA/MSFC Contractor Report), July 1995.

Dale, C. et al., 1994. Spacecraft displacement damage dose calculations for shielded CCDs. Naval Research Laboratory (preprint).

Dudkin, V.E., Potapov, Yu.V., Akopova, A.B., Melkumyan, L.V., Benton, E.V., Frank, A.L., 1990. Differential neutron energy spectra measured on spacecraft in low earth orbit. Nucl. Tracks Radiat. Meas. 17(2), 87.

Dudkin, V.E., Potapov, Yu.V., Akopova, A.B., Melkumyan, L.V., Bogdanov, V.G., Zacharov, V.I., Plyuschev, V.A., Lorabakov, A.P., Lyagyshin, V.I., 1996. Measurements of fast and intermediate neutron energy spectra on Mir space station in the second half of 1991. Radiat. Meas. 26(3), 535.

Griffin, P.J. et al., 1991. Neutron damage equivalence in GaAs. IEEE Trans. Nucl. Sci. 38(6), 1216.

Johnson Space Flight Center, 1994. Space station ionizing radiation design environment. Space Station Program Office, Houston, TX, SSP-30512, February 1994.

ICRP Publication 51, 1987. Data for use in protection against external radiation. Annals of the International Commission on Radiological Protection, Vol. 17, No. 2/3. Pergamon Press, New York.

National Nuclear Data Center, Evaluated Nuclear Data File ENDF/B-V. Brookhaven National Laboratory, Upton, New York.

Tripathi, R.K., Cucinotta, F.A., Wilson, J.W., 1996. Accurate universal parameterization of absorption cross sections. Nucl. Instrum. Methods B 117, 347.